A Structural Model for the Ternary Cleavable Complex Formed between Human Topoisomerase I, DNA, and Camptothecin†

John E. Kerrigan*,‡ and Daniel S. Pilch*,§,||

Department of Pharmaceutical Chemistry, College of Pharmacy, Rutgers-The State University of New Jersey, 160 Frelinghuysen Road, Piscataway, New Jersey 08854-8087, Department of Pharmacology, University of Medicine and Dentistry of New Jersey-Robert Wood Johnson Medical School, 675 Hoes Lane, Piscataway, New Jersey 08854-5635, and The Cancer Institute of New Jersey, New Brunswick, New Jersey 08901

Received May 3, 2001; Revised Manuscript Received June 18, 2001

ABSTRACT: Using the X-ray crystal structure of the human topoisomerase I (TOP1)−DNA cleavable complex, we have developed a general model for the ternary drug−DNA−TOP1 cleavable complex formed with camptothecin (CPT) and its analogues. This model has the drug intercalated between the −1 and +1 base pairs, with the E-ring pointing into the minor groove and the A-ring directed toward the major groove. The ternary complex is stabilized by an array of hydrogen bonding and hydrophobic interactions between the drug and both the enzyme and the DNA. Significantly, the proposed model is consistent with the current body of experimental mutation, cross-linking, and structure−activity data. In addition, the model reveals potential sites of interaction that can provide a rational basis for the design of next generation compounds as well as for de novo drug design.

The DNA topoisomerases have been established as effective molecular targets for anticancer drugs (*1*−*5*). Numerous topoisomerase II (TOP2)[1]-directed drugs have been in clinical use for many years (*4*, *6*). By contrast, only a single family of topoisomerase I (TOP1)-directed drugs has been introduced into the clinic to date (*7*, *8*), namely, the camptothecin (CPT) family of compounds. In animal models, 20(*S*)-CPT (see structure below) and its derivatives have demonstrated a broad spectrum of antineoplastic activity against solid tumors (*9*−*13*).

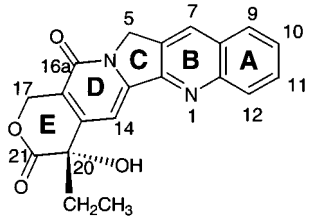

Much effort has been devoted to understanding the molecular basis for this impressive antitumor activity. Interest in TOP1 as an attractive new molecular target for anticancer drugs has stimulated investigations for new TOP1 inhibitors (poisons). These investigations have led to the identification of numerous new compounds that inhibit TOP1, including nitidine (*14*, *15*), the indolocarbazoles (*16*−*19*), the protoberberines (*20*−*22*), the 2-phenylbenzimidazoles (*23*), and the terbenzimidazoles (*24*−*27*). However, despite the increasing number of TOP1 poisons, our current understanding of the molecular mechanism(s) underlying TOP1 inhibition is still quite limited.

The relaxation of superhelical DNA by TOP1 involves repeated cycles of DNA cleavage and religation, with the cleavage step being one of the most critical steps in the catalytic cycle (*28*, *29*). TOP1 poisons are identified and characterized based on their ability to trap the covalent cleavage intermediate, termed the cleavable complex (*30*, *31*). In the case of CPT, stabilization of the cleavage intermediate is the result of specific inhibition of the religation step (*32*, *33*). CPT is a prototypical TOP1 poison that exhibits little or no binding to either DNA or TOP1 alone (*30*, *34*). However, cross-linking studies using alkylating CPT derivatives have indicated that CPT binds to the TOP1−DNA complex (*35*, *36*). Specifically, 10-bromoacetamidomethyl-20(*S*)-CPT was shown to cross-link with the enzyme (*35*), while 7-chloromethyl-10,11-methylenedioxy-20(*S*)-CPT was shown to cross-link to the DNA at the N3 position of the purine base immediately flanking the cleavage site on the 3′-side (the +1 position) (*36*). In both cases, the cleavable complexes became irreversibly trapped. These cross-linking studies suggested that CPT binds to the TOP1−DNA complex at or near the site of DNA cleavage, and have prompted the proposal of two different models for the structural nature of the ternary CPT−DNA−TOP1 cleavable complex; (i) a base flipping model (*37*) and (ii) an interca-

† This work was supported by grants from the American Cancer Society (RPG-99-153-01-C) and the New Jersey Commission on Cancer Research (00-64-CCR-S-0). D.S.P. was supported in part by a Young Investigator Award from The Cancer Institute of New Jersey. J.E.K. was supported by the Charles and Johanna Busch Memorial Fund.

* To whom correspondence should be addressed: Dr. Daniel S. Pilch. Tel.: (732) 235-3352. Fax: (732) 235−4073. E-mail: pilchds@umdnj.edu. Dr. John E. Kerrigan. Tel.: (732) 445-5763. Fax: (732) 445−6312. E-mail: jkerriga@cop.rutgers.edu.

‡ Rutgers University.

§ UMDNJ-Robert Wood Johnson Medical School.

|| The Cancer Institute of New Jersey.

[1] Abbreviations: TOP2, topoisomerase II; TOP1, topoisomerase I; CPT, camptothecin; MD, methylenedioxy; MMFF, Merck molecular force field; MOE, molecular operating environment.

10.1021/bi010913l CCC: $20.00
Published on Web 07/27/2001

lative model (*38*). The base flipping model proposed by Hol and co-workers postulates that the +1 base flips out of the DNA helix and stacks with the drug. The intercalative model proposed by the Pommier group invokes the insertion of the drug between the −1 and +1 base pairs where it interacts favorably with both the DNA and the enzyme (*38*).

Hol and co-workers recently reported a crystal structure of the binary human TOP1−DNA cleavable complex (*37*). This crystal structure affords us the opportunity of using computational techniques to derive structural models of the ternary drug−DNA−TOP1 cleavable complexes that are formed by a broad range of drug families. In this paper, we report structural models for the drug−DNA−TOP1 ternary complexes formed with three CPT analogues, 20(*S*)-CPT, 20(*R*)-CPT, and 10,11-methylenedioxy-20(*S*)-CPT [MD20-(*S*)-CPT]. These models are fully consistent with experimental mutation, cross-linking, and structure−activity data, and establish a rational basis for the design of next generation compounds.

MATERIALS AND METHODS

Preparation of the Crystal Structure of the TOP1−DNA Cleavable Complex. All calculations were performed on a Dell Precision 620 Workstation using the Molecular Operating Environment (MOE; Chemical Computing Group, Inc.). The published X-ray crystal structure of the TOP1−DNA covalent complex (PDB: LA31.PDB) was used as a starting point for development of the model (*37*). Two major modifications were made to this structure: (i) All of the iodouracils were converted to thymines. (ii) The +1 thymine·adenine base pair was converted to a guanine·cytosine base pair. These modifications resulted in the DNA sequence shown below:

```
                          -1 +1
Scissile  5′-AAAAAGACTTT GGAAAAATTTTT-3′
Intact    3′-TTTTTCTGAAA-CCTTTTTAAAAA-5′
```

In addition to the sequence modifications noted above, all the crystallographic water atoms were removed followed by addition of hydrogen atoms to both the enzyme and the DNA. The positions of the hydrogen atoms were energy minimized to a gradient of 0.001 kcal/mol·Å using the Merck molecular force field (MMFF94) (*39*), with the charges on both the protein and the DNA being specified by MMFF94. The entire complex then was minimized to a gradient of 0.1 kcal/mol·Å.

Docking the CPT Derivative into the TOP1−DNA Cleavable Complex. The drugs were each initially geometry optimized using the MMFF94 force field to a gradient of 0.001 kcal/mol·Å. The drug was then placed in the desired orientation and the entire complex was geometry optimized to a gradient of 0.1 kcal/mol·Å. While the positions of the drug ring atoms were fixed during this optimization process, the flexible side chains on the drug were permitted to move freely. The conformational space of the drug in the TOP1−DNA complex was sampled using MOE Dock, a Monte Carlo docking algorithm based on the popular AUTODOCK routine developed at the Scripps Research Institute (*40*, *41*). The upper temperature limit for the docking run was 1000 K. The lowest energy complex resulting from the docking procedure was itself energy minimized using MMFF94 to a gradient of 1.0 kcal/mol·Å. A 12 Å sphere about the drug molecule was further optimized to a gradient of 0.001 kcal/mol·Å. The complexes were ranked using the interaction energies (E_{int}) as the scoring function, with the interaction energy being the sum of the nonbonding interactions [i.e., van der Waals (E_{vdw}) and electrostatic (E_{elec}) contributions] of the complex, as shown below.

$$E_{int} = E_{vdw} + E_{elec}$$

The graphical displays of the models in this report were produced using WebLab ViewerPro (Molecular Simulations, Inc.).

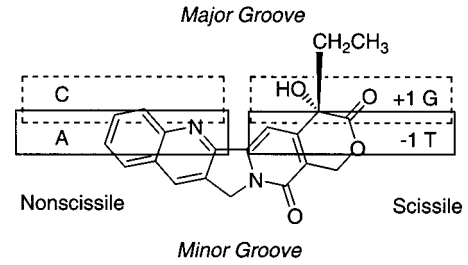

Pommier Intercalation Model

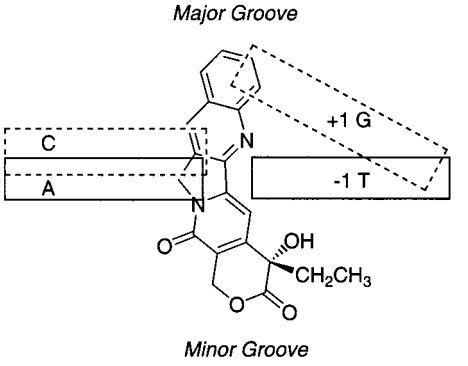

Hol Base-Flipping Model

FIGURE 1: Top views of two previously proposed models for the ternary 20(*S*)-CPT−DNA−TOP1 cleavable complex. The top panel portrays the intercalative model proposed by the Pommier group (*38*), while the bottom panel portrays the base-flipping model proposed by the Hol group (*37*).

RESULTS AND DISCUSSION

Evaluation of Different Orientations for the Docking of 20(S)-CPT into the TOP1−DNA Cleavable Complex. We analyzed six possible orientations for the docking of 20(*S*)-CPT into the TOP1−DNA cleavable complex. Two of these orientations were directed toward the minor groove of the DNA duplex at sites immediately flanking the −1 base pair. However, neither of these binding modes yielded favorable interactions energies in the initial docking calculations. The remaining four drug orientations that we analyzed were intercalative in nature, with the site of intercalation being between the −1 and +1 base pairs.

One of the four intercalative binding orientations we examined was the mode of intercalation previously proposed by Pommier and co-workers (*38*). This binding model (schematically depicted in Figure 1) has the A-ring of the drug pointed directly in toward the DNA backbone of the nonscissile strand. In addition, the Pommier model has the

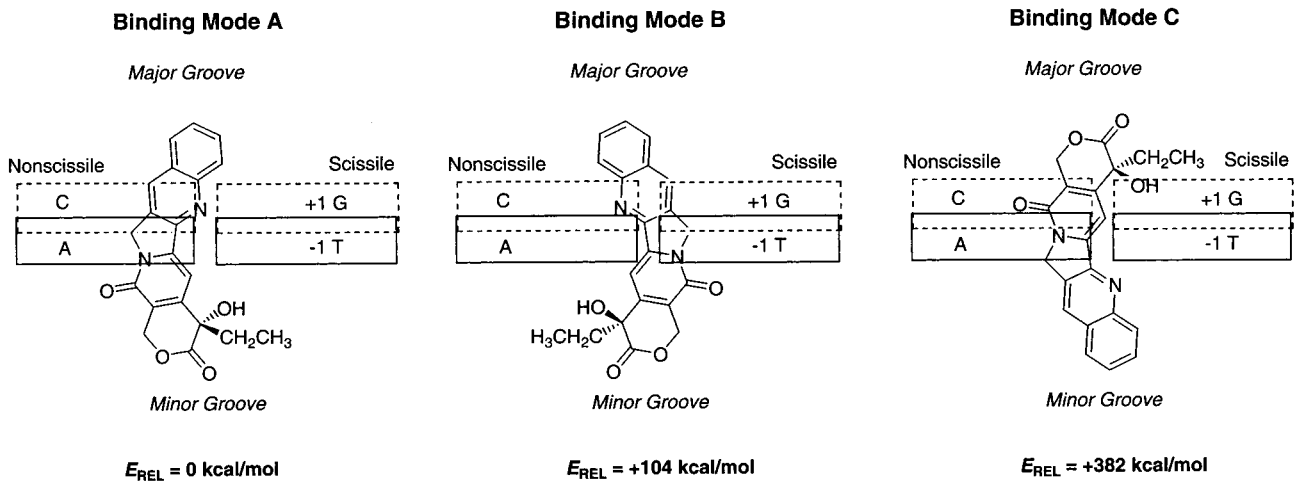

FIGURE 2: Top views of three potential intercalative binding orientations for 20(*S*)-CPT in the ternary 20(*S*)-CPT−DNA−TOP1 cleavable complex. Binding mode A, our proposed intercalative model, yielded the lowest energy structure for the ternary complex, with the relative interaction energies (E_{REL}) of binding modes B and C being higher (less favorable) by 104 and 382 kcal/mol, respectively.

E-ring carbonyl making hydrogen bond contacts to the 6-carbonyl functionality of the +1 guanine on the scissile strand as well as the side chain of the Asn_{722} residue on the enzyme. This latter observation was appealing because it offered a potential molecular explanation for the Asn722Ser mutation that is known to be associated with 20(*S*)-CPT resistance (*42*). Note that the Pommier model was derived before the crystal structure for the TOP1−DNA cleavable complex was reported and, therefore, did not utilize the structural information contained therein. Our attempts to dock 20(*S*)-CPT via the Pommier mode of intercalation failed to yield a stable structure for the ternary drug−DNA−TOP1 complex. Instead, the docking calculations resulted in the drug being displaced into the major groove of the DNA duplex, interacting very little with either the DNA or the enzyme.

In their publication of the crystal structure of the TOP1−DNA cleavable complex, the Hol group proposed a model for the ternary 20(*S*)-CPT−DNA−TOP1 cleavable complex in which the +1 guanine flips out of the DNA helix and stacks with the CPT molecule (*37*). This base flipping model was, in part, based on the following two observations: (i) Photoactivated CPT forms adducts specifically with guanine residues (*43*). (ii) CPT appeared to enhance TOP1-mediated DNA cleavage to the greatest extent when the +1 base was a guanine (*44*). The first of these two observations may be due to guanines having a greater degree of photoreactivity than the other DNA bases rather than to the presence of a specific guanine−CPT interaction. In connection with the second observation, Shen and co-workers (*45*, *46*) have shown that a high percentage of the DNA sites at which CPT stimulates TOP1-mediated cleavage are identical to the sites at which SDS alone stimulates cleavage (i.e., the "background" cleavage sites). Thus, for the majority of DNA sites at which CPT stimulates TOP1-mediated cleavage, the specificity for cleavage at those sites is imparted by TOP1 and not by CPT.

The remaining three intercalative docking orientations we analyzed placed the drug in a perpendicular orientation relative to that in the Pommier model (compare the top panel of Figure 1 with Figure 2). In one of these three orientations (binding mode C in Figure 2), the E-ring is pointed into the major groove, while, in the other two orientations (binding modes A and B), the E-ring is pointed into the minor groove. The difference between binding modes A and B is a 180° rotation about the longitudinal axis of the drug (see Figure 2). Note that all three intercalative binding modes depicted in Figure 2 yielded stable docked structures. However, the interaction energies of these structures differed markedly. Specifically, binding mode A yielded the structure with the lowest energy ($E_{int} = -15\,028$ kcal/mol), with the respective energies of the structures derived from binding modes B and C being 104 and 382 kcal/mol higher in magnitude (i.e., less favorable). On the basis of these differential interaction energies, we selected binding mode A for further investigation.

20(S)-CPT Stabilizes the DNA−TOP1 Cleavable Complex Through Interactions with Both the Enzyme and the DNA. A portion of the final energy minimized structure for the ternary 20(*S*)-CPT−DNA−TOP1 cleavable complex derived from intercalative binding mode A (see Figure 2) is shown in Figure 3. Note that Arg_{364}, Asp_{533}, and Asn_{722} are the closest amino acid residues to the intercalated drug. Arg_{364} and Asp_{533} lie in the DNA minor groove, while Asn_{722} lies on the major groove side of the cleavage site. These amino acid residues, as well as the −1 and +1 base pairs of the DNA, represent the potential sources for favorable interactions with the bound drug. The hydrogen bonding interactions (using a distance cutoff of 3.1 Å) of 20(*S*)-CPT with both the DNA and TOP1 are schematically presented in Figure 4. Inspection of this figure reveals that 20(*S*)-CPT stabilizes the cleavable complex primarily through hydrogen bonding interactions involving its E- and B-rings. Specifically, both the O22 atom and the 21-carbonyl oxygen of the E-ring make multiple hydrogen bonding contacts with Arg_{364}. In addition, the 20-hydroxyl proton is capable of making a hydrogen bond with either the N3 atom of the +1 guanine or a DNA furanose ring oxygen. The N1 atom on the B-ring of 20(*S*)-CPT makes hydrogen bonding contacts to both the 3NH proton of the −1 thymine as well as the 6-NH_2 group of the adenine complement to the −1 thymine. In addition to these hydrogen bonding interactions, stacking interactions between the C-ring of the drug and the adenine complement to the −1 thymine also contribute to the stability of the ternary

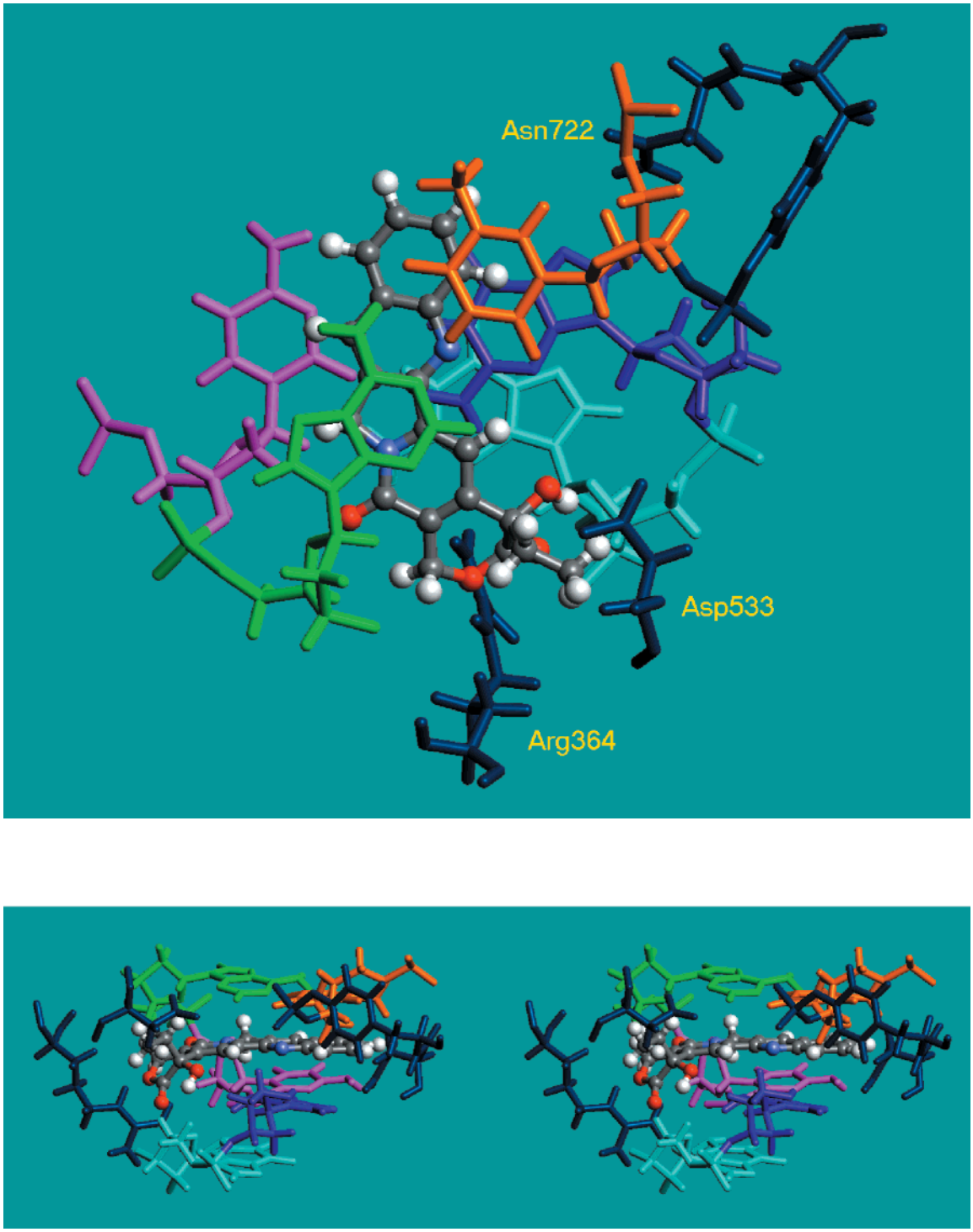

FIGURE 3: A portion of the refined structural model for the ternary 20(*S*)-CPT−DNA−TOP1 cleavable complex. The color coding scheme for the DNA nucleotides is as follows: the −1 thymine orange; the adenine complement to the −1 thymine, green; the +1 guanine, purple; the cytosine complement to the +1 guanine, magenta; the +2 guanine, cyan. The TOP1 amino acid residues are depicted in dark blue, while the 20(*S*)-CPT molecule is depicted according to the following color convention: carbon, gray; oxygen, red; nitrogen, blue; hydrogen, white. The top panel presents a view looking down the DNA helix axis, while the bottom panel presents a stereoview perpendicular to the DNA helix axis.

cleavable complex. In the aggregate, these observations suggest that 20(*S*)-CPT stabilizes the TOP1−DNA cleavable complex through an array of van der Waals and hydrogen bonding interactions with both the enzyme and the DNA.

Correlation of the Proposed Model for the 20(S)-CPT−DNA−TOP1 Cleavable Complex with the Experimental Database. Numerous reported experimental observations are consistent with our proposed structural model for the ternary 20(*S*)-CPT−DNA−TOP1 cleavable complex. These observations include the following: (i) Pommier and co-workers have shown that a 20(*S*)-CPT derivative containing an alkylating functionality at the 7-position of the B-ring forms a cross-link with the N3 atom of the +1 purine base (*36*). Our model of the ternary cleavable complex is consistent with this observation, since it reveals the B-ring of 20(*S*)-CPT to be in proximity to the +1 guanine (see Figure 3).

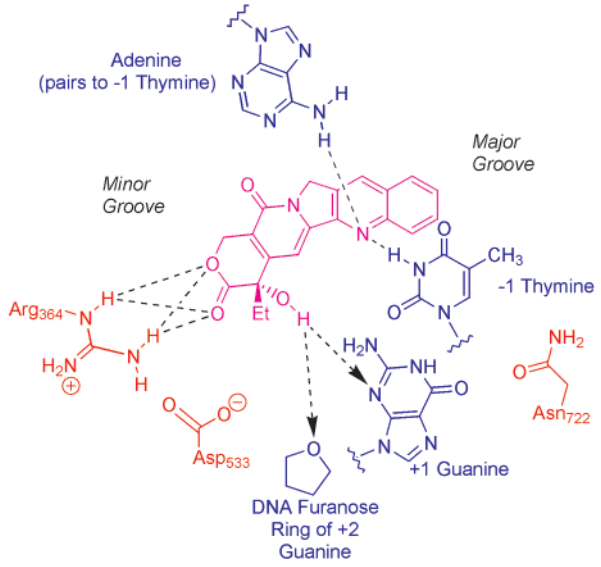

FIGURE 4: A schematic representation of the potential hydrogen bonding contacts between the bound 20(*S*)-CPT molecule and both the DNA and TOP1. The distance cutoff used in the determination of these hydrogen bonding contacts was 3.1 Å. The putative hydrogen bonds are depicted as dashed lines. Note that the dynamics of the 20-hydroxyl moiety are such that it is capable of forming hydrogen bonds with either the N3 atom of the +1 guanine or the DNA furanose ring oxygen atom of the +2 guanine nucleotide. These two potential hydrogen bonds are depicted by dashed arrows. In this figure, DNA functionalities are depicted in blue, TOP1 amino acid residues are depicted in orange, and 20(*S*)-CPT is depicted in magenta.

(ii) Structure−activity studies on CPT derivatives have indicated that the 12-position on the A-ring of 20(*S*)-CPT cannot accommodate bulky substituents without significantly reducing TOP1 poisoning efficacy (*47*). By contrast, bulky substituents at the 7-, 9-, and 10-positions of the drug do not diminish TOP1 poisoning efficacy (*36*, *47*). Our model of the 20(*S*)-CPT−DNA−TOP1 cleavable complex reveals that a bulky substituent at the 12-position would sterically clash with the DNA backbone (see Figure 3). In addition, our model has the 7-, 9-, and 10-positions of 20(*S*)-CPT directed out toward the DNA major groove, where they can accommodate bulky substituents without steric penalty (Figure 3). Hence, the structural features of our model provide explanations for each of the structure−activity relationships noted above.

(iii) Mutations of Arg_{364} (e.g., to His or Gly) are known to cause resistance to CPT (*48*). Our model reveals that hydrogen bonding interactions between Arg_{364} and the E-ring of 20(*S*)-CPT are major stabilizing forces in formation of the ternary CPT−DNA−TOP1 cleavable complex. The disruption of these stabilizing interactions may account for the resistance to CPT associated with the mutation of Arg_{364}. Mutations of Asp_{533} are also known to be associated with CPT resistance (*49*, *50*). In our model of the 20(*S*)-CPT−DNA−TOP1 ternary complex, the Asp_{533} residue of TOP1 is positioned approximately 4.7 Å away from the drug E-ring, a distance that is roughly 1.6 Å out of range for direct hydrogen bonding contact with the drug. However, water molecules could act to form hydrogen bond bridges between Asp_{533} and the 21-carbonyl and/or 20-hydroxyl moieties of the drug. The formation of such water bridge(s) would provide important contributions to the stability of the ternary cleavable complex and may explain why mutations of Asp_{533} lead to CPT resistance (*49*, *50*).

Table 1: Relationship of Relative Interaction Energy (E_{REL}) with Relative TOP1 Cleavage and Cytotoxicity for Three CPT Derivatives

CPT derivative	E_{REL} (kcal/mol)[a]	relative TOP1 cleavage[b]	IC_{50} (μM)[c]
MD20(*S*)-CPT	−24	20	0.027
20(*S*)-CPT	0	1	0.68
20(*R*)-CPT	+454	<0.001	>30

[a] $E_{REL} = E_{Derivative} - E_{20(S)-CPT}$. [b] Normalized relative to 20(*S*)-CPT (*47*). [c] Data taken from Wani et al. (*54*).

(iv) Perhaps the strongest evidence in support of our structural model for the ternary 20(*S*)-CPT−DNA−TOP1 cleavable complex lies in a comparative modeling study we conducted on three different CPT derivatives, 20(*S*)-CPT, 20(*R*)-CPT, and 10,11-methylenedioxy-20(*S*)-CPT [MD20-(*S*)-CPT]. Table 1 summarizes the relative interaction energies (E_{REL}) we determined for the ternary drug−DNA−TOP1 cleavable complexes formed with each of these CPT derivatives, as well as their corresponding TOP1 poisoning and tumor cell killing efficacies. Note that the stabilities of the ternary cleavable complexes formed with the three CPT derivatives correlates with both the TOP1 poisoning and cytotoxic efficacies of these compounds, with each parameter following the hierarchy: MD20(*S*)-CPT > 20(*S*)-CPT ≫ 20(*R*)-CPT. Significantly, our modeling studies provide a molecular basis for this hierarchy. The model of the ternary complex with 20(*R*)-CPT (not shown) reveals an unfavorable steric interaction between the 20-ethyl moiety of the drug and the DNA backbone, which markedly reduces the stability of the ternary complex. By contrast, the model of the ternary complex with MD20(*S*)-CPT (see Figure 5A) indicates that, in addition to making all the interactions previously described for 20(*S*)-CPT, MD20(*S*)-CPT makes additional hydrophobic contacts between its methylenedioxy functionality and the 5-methyl moiety of the −1 thymine (schematically depicted in Figure 5B). Further inspection of Figure 5A reveals that one of the oxygen atoms of the methylenedioxy functionality is approximately 4.5 Å from the side chain of the TOP1 Asn_{722} residue. As noted above in the discussion of Asp_{533}, this distance is roughly 1.4 Å out of range for direct hydrogen bonding contact. However, it is possible for such an interaction to occur via a water bridge (see Figure 5B). Thus, the enhanced TOP1 poisoning efficacy of MD20(*S*)-CPT relative to 20(*S*)-CPT may be the result of additional direct and water-mediated interactions with both the DNA and the enzyme.

(v) A recent meeting abstract reported by Stewart and co-workers (*51*) described a crystal structure of a topotecan−DNA−TOP1 ternary cleavable complex at 2.0 Å resolution. Significantly, this structure was consistent with our model in revealing the intercalation of the drug between the −1 and +1 base pairs as well as a drug-induced displacement of the 5′-end of the scissile strand by ≈3.5 Å downstream from the cleavage site. In addition, the +1 base of the DNA was not rotated (flipped) out of the helix.

CONCLUDING REMARKS

We have used the X-ray crystal structure of the TOP1−DNA cleavable complex to derive structural models for

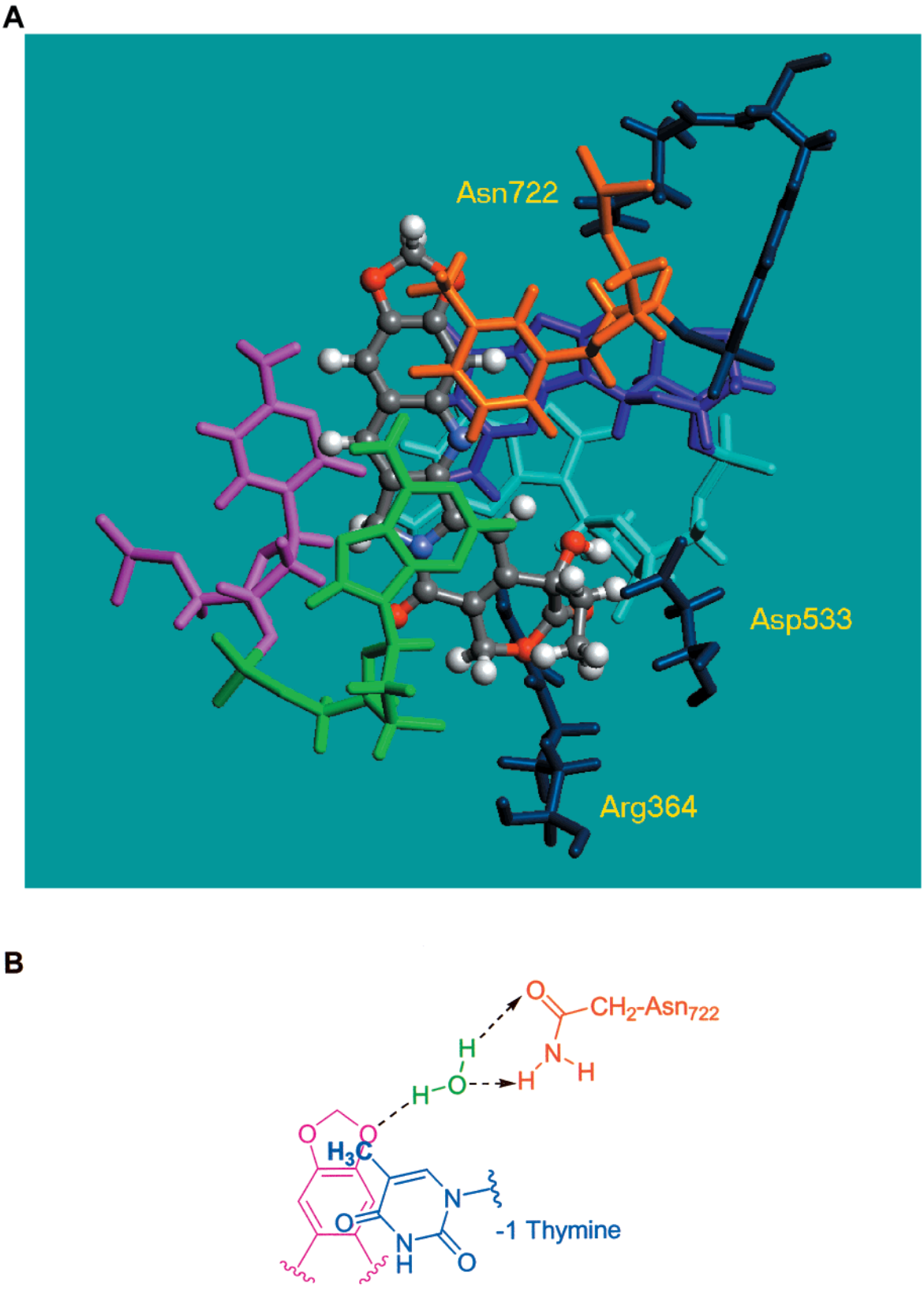

FIGURE 5: (A) A portion of the refined structural model for the ternary MD20(*S*)-CPT−DNA−TOP1 cleavable complex presented as a top view looking down the DNA helix axis. The color coding scheme is the same as in Figure 3. (B) A schematic representation of the potential hydrophobic and hydrogen bonding contacts involving the methylenedioxy functionality of MD20(*S*)-CPT. Note that in addition to hydrophobic interactions between the methylenedioxy group and the 5-methyl moiety of the −1 thymine, water-mediated hydrogen bonding contacts between the methylenedioxy group and the TOP1 Asn_{722} residue are also possible (depicted as dashed lines and arrows). The color coding scheme in this panel is identical to that in Figure 4, with the addition of a water molecule in green.

ternary CPT−DNA−TOP1 cleavable complexes that are fully consistent with the current experimental database. Although numerous aspects of our gas phase models are fully consistent with existing experimental data, we recognize that water molecules can play an important role in modulating ligand-macromolecule recognition (*52*, *53*). Consequently,

future efforts will be directed toward refining our models of the CPT−DNA−TOP1 cleavable complexes to include the effects of solvation. Nevertheless, the models presented in this report provide insight into the specific molecular interactions that stabilize the ternary cleavable complexes. In addition, the models reveal potential sites of interaction that can provide a rational basis for the design of next generation compounds as well as for de novo drug design.

ACKNOWLEDGMENT

We thank Drs. Leroy F. Liu and Edmond J. LaVoie for helpful discussions.

REFERENCES

1. Liu, L. F. (1989) *Annu. Rev. Biochem. 58*, 351−375.
2. D'Arpa, P., and Liu, L. F. (1989) *Biochim. Biophys. Acta 989*, 163−177.
3. Pommier, Y. (1993) *Cancer Chemother. Pharmacol. 32*, 103−108.
4. Chen, A. Y., and Liu, L. F. (1994) *Annu. Rev. Pharmacol. Toxicol. 34*, 191−218.
5. Liu, L. F. (1994) in *Advances in Pharmacology*, Academic Press, San Diego.
6. Bodley, A. L., and Liu, L. F. (1988) *Bio/Technology 6*, 1315−1319.
7. Slichenmeyer, W. J., Rowinsky, E. K., Donehower, R. C., and Kaufmann, S. H. (1993) *J. Natl. Cancer Inst. 85*, 271−291.
8. Potmesil, M. (1994) *Cancer Res. 54*, 1431−1439.
9. Giovanella, B. C., Stehlin, J. S., Wall, M. E., Wani, M. C., Nicholas, A. W., Liu, L. F., Silber, R., and Potmesil, M. (1989) *Science 246*, 1046−1048.
10. Giovanella, B. C., Hinz, H. R., Kozielski, A. J., Stehlin, A. J., Jr., Silber, R., and Potmesil, M. (1991) *Cancer Res. 51*, 3052−3055.
11. Pantazis, P., Hinz, H. R., Mendoza, J. T., Kozielski, A. J., Williams, L. J., Stehlin, J. S., and Giovanella, B. C. (1992) *Cancer Res. 52*, 3980−3987.
12. Pantazis, P., Early, J. A., Kozielski, A. J., Mendoza, J. T., Hinz, H. R., and Giovanella, B. C. (1993) *Cancer Res. 53*, 1577−1582.
13. Pantazis, P., Kozielski, A. J., Mendoza, J. T., Early, J. A., Hinz, H. R., and Giovanella, B. C. (1993) *Int. J. Cancer 53*, 863−871.
14. Wang, L.-K., Johnson, R. K., and Hecht, S. M. (1993) *Chem. Res. Toxicol. 6*, 813−818.
15. Holden, J. A., Wall, M. E., Wani, M. C., and Manikumar, G. (1999) *Arch. Biochem. Biophys. 370*, 66−76.
16. Yamashita, Y., Fujii, N., Murakata, C., Ashizawa, T., Okabe, M., and Nakano, H. (1992) *Biochemistry 31*, 12069−12075.
17. Yoshinari, T., Yamada, A., Uemura, D., Nomura, K., Arakawa, H., Kojiri, K., Yoshida, E., Suda, H., and Okura, A. (1993) *Cancer Res. 53*, 490−494.
18. Kanzawa, F., Nishio, K., Kubota, N., and Saijo, N. (1995) *Cancer Res. 55*, 2806−2813.
19. Bailly, C., Riou, J.-F., Colson, P., Houssier, C., Rodrigues-Pereira, E., and Prudhomme, M. (1997) *Biochemistry 36*, 3917−3929.
20. Makhey, D., Gatto, B., Yu, C., Liu, A., Liu, L. F., and LaVoie, E. J. (1995) *Med. Chem. Res. 5*, 1−12.
21. Makhey, D., Gatto, B., Yu, C., Liu, A., Liu, L. F., and LaVoie, E. J. (1996) *Bioorg. Med. Chem. 4*, 781−791.
22. Gatto, B., Sanders, M. M., Yu, C., Wu, H.-Y., Makhey, D., LaVoie, E. J., and Liu, L. F. (1996) *Cancer Res. 56*, 2795−2800.
23. Kim, J. S., Sun, Q., Gatto, B., Yu, C., Liu, A., Liu, L. F., and LaVoie, E. J. (1996) *Bioorg. Med. Chem. 4*, 621−630.
24. Sun, Q., Gatto, B., Yu, C., Liu, A., Liu, L. F., and LaVoie, E. J. (1995) *J. Med. Chem. 38*, 3638−3644.
25. Kim, J. S., Yu, C., Liu, A., Liu, L. F., and LaVoie, E. J. (1997) *J. Med. Chem. 40*, 2818−2824.
26. Kim, J. S., Sun, Q., Yu, C., Liu, A., Liu, L. F., and LaVoie, E. J. (1998) *Bioorg. Med. Chem. 6*, 163−172.
27. Rangarajan, M., Kim, J. S., Jin, S., Sim, S.-P., Liu, A., Pilch, D. S., Liu, L. F., and LaVoie, E. J. (2000) *Bioorg. Med. Chem. 8*, 1371−1382.
28. Wang, J. C. (1985) *Annu. Rev. Biochem. 54*, 665−697.
29. Champoux, J. J. (1994) *Adv. Pharmacol. 29A*, 71−82.
30. Hsiang, Y.-H., Hertzberg, R., Hecht, S., and Liu, L. F. (1985) *J. Biol. Chem. 260*, 14873−14878.
31. Champoux, J. J. (1977) *Proc. Natl. Acad. Sci. U.S.A. 74*, 3800−3804.
32. Porter, S. E., and Champoux, J. J. (1989) *Nucleic Acids Res. 17*, 8521−8532.
33. Svejstrup, J. Q., Christiansen, K., Gromova, I. I., Andersen, A. H., and Westergaard, O. (1991) *J. Mol. Biol. 222*, 669−678.
34. Hertzberg, R. P., Caranfa, M. J., and Hecht, S. M. (1989) *Biochemistry 28*, 4629−4638.
35. Hertzberg, R. P., Busby, R. W., Caranfa, M. J., Holden, K. G., Johnson, R. K., Hecht, S. M., and Kingsbury, W. D. (1990) *J. Biol. Chem. 265*, 19287−19295.
36. Pommier, Y., Kohlhagen, G., Kohn, K. W., Leteurtre, F., Wani, M. C., and Wall, M. E. (1995) *Proc. Natl. Acad. Sci. U.S.A. 92*, 8861−8865.
37. Redinbo, M. R., Stewart, L., Kuhn, P., Champoux, J. J., and Hol, W. G. J. (1998) *Science 279*, 1504−1513.
38. Fan, Y., Weinstein, J. N., Kohn, K. W., Shi, L. M., and Pommier, Y. (1998) *J. Med. Chem. 41*, 2216−2226.
39. Halgren, T. A. (1996) *J. Comput. Chem. 17*, 490−519.
40. Goodsell, D. S., and Olson, A. J. (1990) *Proteins 8*, 195−202.
41. Goodsell, D. S., Morris, G. M., and Olson, A. J. (1996) *J. Mol. Recognit. 9*, 1−5.
42. Fujimori, A., Harker, W. G., Kohlhagen, G., Hoki, Y., and Pommier, Y. (1995) *Cancer Res. 55*, 1339−1346.
43. Leteurtre, F., Fesen, M., Kohlhagen, G., Kohn, K. W., and Pommier, Y. (1993) *Biochemistry 32*, 8955−8962.
44. Kjeldsen, E., Mollerup, S., Thomsen, B., Bonven, B. J., Bolund, L., and Westergaard, O. (1988) *J. Mol. Biol. 202*, 333−342.
45. Perez-Stable, C., Shen, C. C., and Shen, C.-K. J. (1988) *Nucleic Acids Res. 16*, 7975−7993.
46. Shen, C. C., and Shen, C.-K. J. (1990) *J. Mol. Biol. 212*, 67−78.
47. Hsiang, Y.-H., Liu, L. F., Wall, M. E., Wani, M. C., Nicholas, A. W., Manikumar, G., Kirschenbaum, S., Silber, R., and Potmesil, M. (1989) *Cancer Res. 49*, 4385−4389.
48. Pommier, Y., Pourquier, P., Urasaki, Y., Wu, J., and Laco, G. S. (1999) *Drug Resist. Updates 2*, 307−318.
49. Andoh, T., Ishii, K., Suzuki, Y., Ikegami, Y., Kusunoki, Y., Takemoto, Y., and Okada, K. (1987) *Proc. Natl. Acad. Sci. U.S.A. 84*, 5565−5569.
50. Tamura, H.-O., Kohchi, C., Yamada, R., Ikeda, T., Koiwai, O., Patterson, E., Keene, J. D., Okada, K., Kjeldsen, E., and Nishikawa, K. (1991) *Nucleic Acids Res. 19*, 69−75.
51. Stewart, L., Staker, B., Hjerrid, K., Burgin, A. J., and Kim, H. (2001) in *92nd Annual Meeting of the American Association for Cancer Research*, pp S80−S81, New Orleans, LA.
52. Chalikian, T. V., Plum, G. E., Sarvazyan, A. P., and Breslauer, K. J. (1994) *Biochemistry 33*, 8629−8640.
53. Qu, X., and Chaires, J. B. (2000) *J. Am. Chem. Soc. 123*, 1−7.
54. Wani, M. C., Nicholas, A. W., and Wall, M. E. (1986) *J. Med. Chem. 29*, 2358−2363.

BI010913L